ResearchGate

See discussions, stats, and author profiles for this publication at: https://www.researchgate.net/publication/326586084

Mobile Robot Localization Considering Class of Sensor Observations

Conference Paper · October 2018

DOI: 10.1109/IROS.2018.8594146

CITATIONS
7

READS
833

3 authors:

Naoki Akai
Nagoya University
62 PUBLICATIONS **254** CITATIONS
SEE PROFILE

Y. Morales
Standard Cognition
95 PUBLICATIONS **878** CITATIONS
SEE PROFILE

H. Murase
Nagoya University
367 PUBLICATIONS **8,317** CITATIONS
SEE PROFILE

Some of the authors of this publication are also working on these related projects:

face recognition View project

Personal Mobility Vehicle Shared Control and Automation View project

All content following this page was uploaded by Naoki Akai on 25 July 2018.

The user has requested enhancement of the downloaded file.

Mobile Robot Localization Considering Class of Sensor Observations

Naoki Akai[1], Luis Yoichi Morales[1], and Hiroshi Murase[2]

***Abstract*— Localization robustness against environment dynamics is significant for robots to achieve autonomous navigation in unmodified environments. A basic method of improving the robustness of a robot is considering the sensor observations obtained from mapped obstacles and using them for localizing the robot's pose. This study proposes an observation model that considers the class of sensor observations, where "class" categorizes the sensor observations as those obtained from mapped and unmapped obstacles. In the proposed approach, the robot's pose and the class are estimated simultaneously. As a result, the robot's pose can be localized using the sensor observations obtained only from mapped obstacles. First, we evaluated the performance of the proposed approach using simulations. Further, we tested the proposed approach in a real-world mobile robot navigation competition, called "Tsukuba Challenge," held in Japan. The robustness and effectiveness of the proposed approach against environment dynamics were verified from the experimental results.**

I. Introduction

Localization robustness against environment dynamics is important to achieve autonomous navigation in unmodified environments. Furthermore, localization-based autonomous navigation has already been achieved, as discussed in [1], [2], [3]. However, achieving robustness against environment dynamics is still a significant concern for the localization process. To improve robustness, the following two approaches can be considered as effective approaches: 1) recognizing the dynamics and adaptively updating the map, and 2) applying an observation model that can correspond to the dynamics. This study proposes an observation model that considers the class of sensor observations, where "class" categorizes the sensor observations as those obtained from mapped and unmapped obstacles. In other words, the proposed approach allows a robot to localize its pose using the sensor observations obtained only from mapped obstacles.

Figure 1 illustrates a scene of our target mobile robot navigation test. The robot is equipped with a two-dimensional (2D) light detection and ranging (LiDAR) device, and has an environment map for localizing its pose. The robot was navigating in a real city environment; thus, many dynamic obstacles, such as pedestrians and bicycles, passed around the robot. In addition, small bumps on the ground surface produced vibrations in the robot's roll and pitch angles, which led to noisy observations. To robustly localize the robot's pose under such conditions, accurately distinguishing the sensor observations class is effective. As shown in the bottom figure of Fig. 1, the proposed approach allows the robot to distinguish the class and the robot's pose is localized using the sensor observations obtained only from mapped obstacles. Although the proposed approach estimates the robot's pose and the class simultaneously, it does not affect the computation complexity, i.e., it is the same as that from the original Monte Carlo localization (MCL) presented in [4], [5].

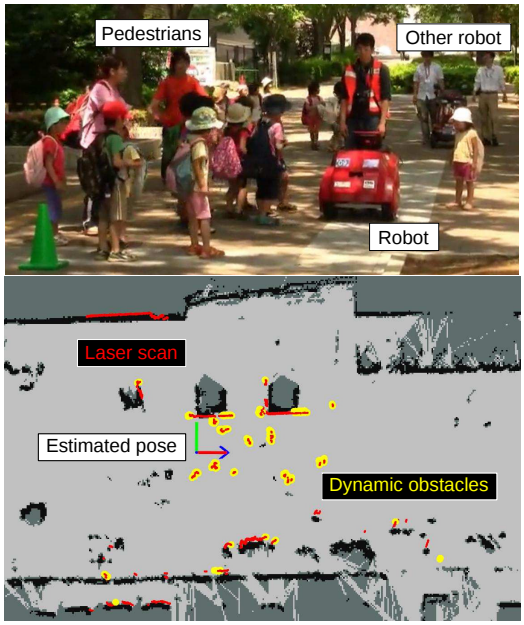

Fig. 1. Autonomous navigation in a dynamic city environment (top). The proposed approach distinguishes between the sensor observations obtained from mapped and unmapped obstacles. In the bottom figure, the original laser scan data are depicted with red points and observations obtained from unmapped obstacles are shown with yellow points.

The contributions of this study are summarized as follows:

- An observation model is proposed that considers the class of sensor observations.
- Robust localization is achieved without increasing the computation complexity.

The remainder of this study is organized as follows. Section II summarizes the related works. Section III describes the proposed approach. Section IV describes the implementation of the proposed approach. Section V evaluates the proposed approach using simulated and actual robots. Section VI concludes our study.

II. Related works

Generally, mobile robot localization and mapping problems are considered assuming the environment to be static, which is not a suitable assumption for robots working in real

[1]Naoki Akai and Luis Yoichi Morales are with the Institute of Innovation for Future Society (MIRAI), Nagoya University, Nagoya 464-8601, Japan {akai, morales_yoichi}@coi.nagoya-u.ac.jp

[2]Hiroshi Murase is with the Graduate School of Information Science, Nagoya University, Nagoya 464-8603, Japan murase@nagoya-u.jp

environments. Thus, dynamic environment localization and mapping have been widely studied.

The major dynamics in real world mobile robot navigation are obstacles, such as pedestrians, bicycles, and cars. The simplest method of improving robustness against such highly dynamic obstacles is to treat them as outlier [6], [7], [8], [9], [10], [11]. This approach works well for such highly dynamic obstacles; however, it is not effective for semi-dynamic obstacles, which are obstacles that are not always moving, e.g., parked cars. For coping with both dynamic and semi-dynamic obstacles, several approaches have been proposed.

One such effective method is to create an observation model that robustly calculates the likelihoods under dynamic environments. Olufs *et al*. and Takeuchi *et al*. proposed similar observation models [12], [13]. In this approach, the free space, from where the laser beams pass, is used for robustly calculating the likelihoods. However, this approach does not work in areas with one side open because of the characteristic of the models. Our proposed approach works in such areas and accurately calculates the likelihoods under dynamic environments.

Approaches that specifically focused on separating the static and dynamic aspects of the environments by building two maps were also proposed. Wolf *et al*. proposed a model that maintained two separate occupancy grids, one each for the static and dynamic parts [14]. Montesano *et al*. extended this approach by considering the problems of dynamic object detection and mapping simultaneously, and including the error estimation of the robot in the classifier [15]. Biber *et al*. proposed a model that represented an environment on multiple timescales simultaneously to select the sensor data of the most appropriate timescale. Wang *et al*. formulated a general framework for dynamic object detection, mapping, and tracking by employing a system to detect if a measurement is caused by a dynamic object [17]. Gallagher *et al*. built maps for individual objects that could then be overlaid to represent the current configuration of the environment [18]. The main advantage of these approaches over filtering dynamic observations is that they are able to provide a better static map of the environment and dynamic observations can be detected more reliably. However, they still face the same limitations of the static world assumptions when deployed in changing environments or where the dynamics are low.

To overcome the limitations due to the static world assumptions, some researchers worked on how to model the environment dynamics as a single unified representation. Chen *et al*. and recently Brechtel *et al*. extended the occupancy grid paradigm to include moving objects [19], [20]. Meyer-Delius *et al*. proposed a dynamic occupancy grid, which employs hidden Markov models on a 2D grid to represent the occupancy and its dynamics [21]. Saarinen *et al*. proposed to model the environment as a set of independent Markov chains, one per grid cell, each with two states [22]. The main advantage of these approaches over modeling the environment dynamics is that the map used for localization can be adaptively updated and the robot's pose is robustly localized against dynamic obstacles. However, a complex computation process like simultaneous localization and mapping (SLAM) using a Rao-Blackwellized particle filter (RBPF) is required to employ the dynamic map representation for localizing the robot's pose.

To handle the complexity of the RBPF solution in practical applications, some researchers proposed to focus on only some dynamic aspects or restrict the dynamics to a set of static configurations. Avots *et al*. used the RBPF to estimate the robot's pose and the state of doors in the environment [23]. They represented the environment using an occupancy grid, in which the location of the doors is known, but not their state, i.e., opened or closed. Petrovskaya *et al*. proposed a similar approach, in which instead of a binary model, a parametrized model (opening angle) of the doors is used [24]. Stachniss *et al*. clustered local grid maps to identify a set of possible configurations of an environment [25]. The RBPF is then used to localize the robot's pose and estimate the configuration of the environment from the set. Milstein [26] used the RBPF to estimate the robot's pose and update the environment map represented by an occupancy grid. Tipaldi *et al*. proposed an approach that estimated the state of the complete environment, and not only of a small, specific area or element [27]. Additionally, the approach also learns the model parameters from data and is able to generalize over unforeseen environment configurations. To employ the RPBF-based map updation approaches, each particle must have the map data, which always causes the memory limitation problem when in a large environment. Our proposed approach uses only one map data and avoids the memory problem.

Instead of updating a reference map, Valencia *et al*. proposed the use of dual timescale (short and long terms) maps for localization in highly dynamic environment [28]. This approach could use semi-dynamic obstacles for localizing the robot's pose, because the short-term timescale map could record them as landmarks. However, re-localizing is significantly difficult once an estimation fails because the mapping process considering a short-term timescale map will fail and localization is significantly affected by the miss-mapping result.

The approach proposed in this study is similar to the research works presented in [29], [30]. In [29], the objective was set to estimate the distribution of the robot's pose and the semi-static obstacle map simultaneously. By simultaneously estimating them, semi-static obstacles could be used for localizing the robot's pose. Moreover, our objective is to estimate the distribution of the robot's pose and class of the sensor observations simultaneously. Thus, we could not use semi-static obstacles for localizing the robot's pose. However, it improves the localization robustness against dynamic obstacles because the scan observations obtained from dynamic obstacles are not affected while localizing the robot's pose. In [30], two types of observation models considering the static and moving obstacles were used, and these models were calculated based on the feasibility grids. In our approach, two types of conditional observation

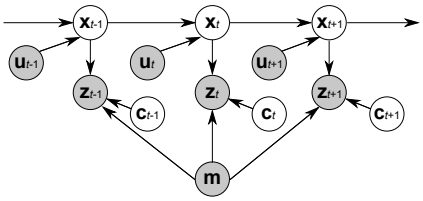

Fig. 2. Graphical model used in the proposed approach.

models are used; however, no other information is used to calculate them. Nevertheless, the localization robustness against dynamic obstacles is improved.

III. Proposed approach

Figure 2 illustrates the graphical model used in the proposed approach. In this figure, the hidden and observable variables are shown with white and gray nodes, respectively. We have sensor observations $\mathbf{z}$, control inputs $\mathbf{u}$, and map $\mathbf{m}$ as observable variables, and poses of a robot $\mathbf{x}$, and classes of sensor observations $\mathbf{c}$ as hidden variables.

Our objective is to estimate the joint probabilistic distribution denoted as

$$p(\mathbf{x}_t, \mathbf{c}_t | \mathbf{z}_{1:t}, \mathbf{u}_{1:t}, \mathbf{m}), \tag{1}$$

where t is the time index and $1:t$ represents the time series data. We apply the multiplication theorem to Equation (1), and it can be expressed as

$$\begin{aligned} &p(\mathbf{x}_t, \mathbf{c}_t | \mathbf{z}_{1:t}, \mathbf{u}_{1:t}, \mathbf{m}) \\ &= p(\mathbf{x}_t | \mathbf{z}_{1:t}, \mathbf{u}_{1:t}, \mathbf{m}) p(\mathbf{c}_t | \mathbf{x}_t, \mathbf{z}_{1:t}, \mathbf{u}_{1:t}, \mathbf{m}). \end{aligned} \tag{2}$$

First, we focus on the second term on the right-hand side of Equation (2). Bayes' theorem can be applied using a sensor observation $\mathbf{z}_t$, and it can be expressed as

$$\begin{aligned} &p(\mathbf{c}_t | \mathbf{x}_t, \mathbf{z}_{1:t}, \mathbf{u}_{1:t}, \mathbf{m}) \\ &= \eta p(\mathbf{z}_t | \mathbf{x}_t, \mathbf{c}_t, \mathbf{z}_{1:t-1}, \mathbf{u}_{1:t}, \mathbf{m}) p(\mathbf{c}_t | \mathbf{x}_t, \mathbf{z}_{1:t-1}, \mathbf{u}_{1:t}, \mathbf{m}), \end{aligned} \tag{3}$$

where η is the normalization constant (η is used as a normalization constant in this study). Further, Markov property is applied, and the following equation is obtained:

$$\begin{aligned} &\eta p(\mathbf{z}_t | \mathbf{x}_t, \mathbf{c}_t, \mathbf{z}_{1:t-1}, \mathbf{u}_{1:t}, \mathbf{m}) p(\mathbf{c}_t | \mathbf{x}_t, \mathbf{z}_{1:t-1}, \mathbf{u}_{1:t}, \mathbf{m}) \\ &= \eta p(\mathbf{z}_t | \mathbf{x}_t, \mathbf{c}_t, \mathbf{m}) p(\mathbf{c}_t), \end{aligned} \tag{4}$$

where $p(\mathbf{z}_t | \mathbf{x}_t, \mathbf{c}_t, \mathbf{m})$ and $p(\mathbf{c}_t)$ are the likelihood and prior distributions considering the class. We do not use an object tracking function; thus, it is impossible to determine the prior distribution[1]. Therefore, we assume that the prior distribution is constant. It should be noted that we can obtain computational efficiency by this assumption; however, it does not affect the performance.

In the proposed approach, elements of the class $\mathbf{c} = ({}^1c, {}^2c, ..., {}^Kc)^T$ are corresponding to each element of the sensor observation $\mathbf{z} = ({}^1\mathbf{z}, {}^2\mathbf{z}, ..., {}^K\mathbf{z})^T$, where we assume that each sensor observation is independent. Thus, Equation (4) can be rewritten as

$$\eta p(\mathbf{z}_t | \mathbf{x}_t, \mathbf{c}_t, \mathbf{m}) p(\mathbf{c}_t) = \eta \prod_{i=1}^{K} p({}^i\mathbf{z}_t | \mathbf{x}_t, {}^i c_t, \mathbf{m}) p({}^i c_t), \tag{5}$$

where $p({}^i\mathbf{z}_t | \mathbf{x}_t, {}^i c_t, \mathbf{m})$ is an observation model with a condition in which the class of the sensor observation is given. We refer it as "conditional observation model" in this study. This model is discussed in detail in Section IV.

Further, we focus on the first term on the right-hand side of Equation (2). This term is well known in the localization problem and it can be expressed as the following recursive equation:

$$\begin{aligned} &p(\mathbf{x}_t | \mathbf{z}_{1:t}, \mathbf{u}_{1:t}, \mathbf{m}) = \eta p(\mathbf{z}_t | \mathbf{x}_t, \mathbf{m}) \\ &\int p(\mathbf{x}_t | \mathbf{x}_{t-1}, \mathbf{u}_t) p(\mathbf{x}_{t-1} | \mathbf{z}_{1:t-1}, \mathbf{u}_{1:t-1}, \mathbf{m}) d\mathbf{x}_{t-1}, \end{aligned} \tag{6}$$

where $p(\mathbf{z}_t | \mathbf{x}_t, \mathbf{m})$ and $p(\mathbf{x}_t | \mathbf{x}_{t-1}, \mathbf{u}_t)$ are the observation and motion models. In the proposed approach, we have the hidden variable $\mathbf{c}_t$ and can apply the law of total probability to the observation model

$$p(\mathbf{z}_t | \mathbf{x}_t, \mathbf{m}) = \int p(\mathbf{z}_t | \mathbf{x}_t, \mathbf{c}_t, \mathbf{m}) p(\mathbf{c}_t) d\mathbf{c}_t. \tag{7}$$

The assumption that each sensor observation is independent can be also applied to this equation, and the observation model is rewritten as

$$p(\mathbf{z}_t | \mathbf{x}_t, \mathbf{m}) = \prod_{i=1}^{K} \int p({}^i\mathbf{z}_t | \mathbf{x}_t, {}^i c_t, \mathbf{m}) p({}^i c_t) d^i c_t. \tag{8}$$

Before calculating this equation, the distribution shown in Equation (3) can be calculated. Further, the calculation result of Equation (3) can be applied to compute Equation (8). As a result, the proposed approach can localize the robot's pose considering the sensor observation class.

IV. Implementation

To estimate the objective distribution shown in Equation (1), we use an RBPF. In the RBPF, the robot's pose is estimated based on a sampling-based method, and the sensor observation class is analytically calculated. It should be noted that the computation complexity of the RBPF is the same as that of the original MCL because the analytical calculation part can be computed with the same timing as that required for calculating the importance weight of the particles. This section discussed in detail the observation model expressed in Equation (8).

A. Class of sensor observations

In this study, two states are used as the sensor observation class, $C = \{\mathrm{mapped}, \mathrm{unmapped}\}$, where mapped and $\mathrm{unmapped}$ refer to mapped and unmapped obstacles, respectively, on the given map. To calculate the observation model, the prior distribution regarding the class, $p({}^i c_t)$, should be estimated first. However, this distribution cannot be estimated because object tracking is not employed in this study. Thus, we assume that this prior distribution is constant, i.e., $p(c_t = \mathrm{mapped}) = p(c_t = \mathrm{unmapped}) = 0.5$.

[1] $\mathbf{c}_t$ and $\mathbf{c}_{t-1}$ can be connected in the graphical model if object tracking is applied, and then the prior distribution can be estimated.

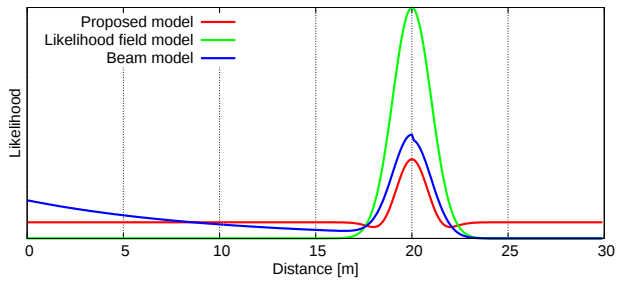

Fig. 3. Shape comparison result of observation models.

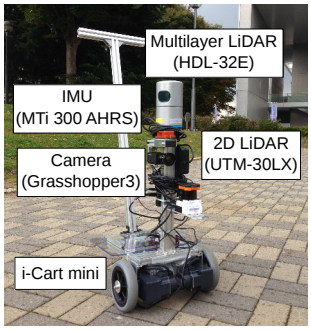

Fig. 4. Data collection platform.

B. Conditional observation model

To define the conditional observation model in which the mapped observation class is given as the condition, we use the likelihood field model (LFM) [5] denoted as

$$p({}^i\mathbf{z}_t|\mathbf{x}_t, {}^i c_t = \text{mapped}, \mathbf{m}) \tag{9}$$
$$= \begin{pmatrix} z_{\text{hit}} \\ z_{\text{max}} \\ z_{\text{rand}} \end{pmatrix}^T \cdot \begin{pmatrix} p_{\text{hit}}({}^i\mathbf{z}_t|\mathbf{x}_t, \mathbf{m}) \\ p_{\text{max}}({}^i\mathbf{z}_t|\mathbf{x}_t, \mathbf{m}) \\ p_{\text{rand}}({}^i\mathbf{z}_t|\mathbf{x}_t, \mathbf{m}) \end{pmatrix},$$

where z_{hit}, z_{max}, and z_{rand} are the weight factors, they must satisfy the following condition: $z_{\text{hit}} + z_{\text{max}} + z_{\text{rand}} = 1$, and p_{hit}, p_{max}, and p_{rand} are the probabilistic distributions in terms of hitting the mapped obstacles, measuring the maximum sensor measurement, and measuring random measurements, respectively. These details can be found in [5].

The conditional observation model for which the unmapped observation class is given is denoted as

$$p({}^i\mathbf{z}_t|\mathbf{x}_t, {}^i c_t = \text{unmapped}, \mathbf{m}) \tag{10}$$
$$= \eta \left(\max_{\text{mapped}} - p({}^i\mathbf{z}_t|\mathbf{x}_t, {}^i c_t = \text{mapped}, \mathbf{m})\right),$$

where $\max_{\text{mapped}}$ is the maximum value of the distribution $p({}^i\mathbf{z}_t|\mathbf{x}_t, {}^i c_t = \text{mapped}, \mathbf{m})$. Finally, the observation model used in the proposed approach is denoted as

$$\prod_{i=1}^{K} \int p({}^i\mathbf{z}_t|\mathbf{x}_t, {}^i c_t, \mathbf{m}) p({}^i c_t) d^i c_t = \tag{11}$$
$$\prod_{i=1}^{K} (p({}^i\mathbf{z}_t|\mathbf{x}_t, {}^i c_t = \text{mapped}, \mathbf{m}) p({}^i c_t = \text{mapped}) +$$
$$p({}^i\mathbf{z}_t|\mathbf{x}_t, {}^i c_t = \text{unmapped}, \mathbf{m}) p({}^i c_t = \text{unmapped})).$$

Figure 3 shows the result of shape comparison with three observation models: proposed model, LFM, and beam model (BM). The details about the LFM and BM are available in [5]. A landmark is located at a distance of 20 m. The distribution characteristic by the proposed approach is to have small likelihood throughout the possible range. Thus, the likelihood of the particles can be robustly calculated against dynamic obstacles.

V. Evaluation

This section evaluates the proposed approach using simulated and actual robots. In the simulation experiments, we reproduced the specification same as that of an actual robot. In the actual environment experiments, we took log data using the robot in the Tsukuba Challenge (TC)[2] 2017's environment and evaluated the approach off-line.

A. Experimental platform

Figure 4 shows the robot used in the actual environment experiments. This robot is installed with a 2D LiDAR, multilayer LiDAR, camera, inertial measurement unit (IMU), and encoders. To implement the proposed approach, the 2D LiDAR, IMU, and encoders were used. The specification of the 2D LiDAR are as follows. The maximum measurement range is 30 m, scan angle range is 270 degress, and scan angle resolution is 0.25 degress.

B. Methods used for comparison

The proposed approach was compared with four methods: LFM with and without the rejection method, and BM with and without the rejection method; where the rejection method refers to an algorithm used for rejecting the scan points obtained from unmapped objects[3]. Each comparison method is notated as LFMwRM, LFMwoRM, BMwRM, and BMwoRM in this section.

C. Simulation experiments

1) Likelihood distribution: First, we focused on the likelihood distributions generated using each observation model. In the experiments, we simulated the moving obstacles that move randomly and deleted some static landmarks randomly for validating the robustness against environment dynamics.

Figure 5 shows the two comparison results in Figs. 5(a) and 5(b). The top left figures show the simulated environment. The simulation map (green), used for simulating the 2D scan, was created by removing the static landmarks from approximately 90 % of the landmark map (red) used for calculating the likelihood distributions. The blue dots represent the current scan measurement plotted from the ground truth, $(x, y, \theta) = (0, 0, 0)$. In each experiment, approximately 10 % of the scan data was obtained from the landmarks and the remaining scan data was obtained from the dynamic obstacles.

[2]Details about Tsukuba Challenge can be found at `http://www.tsukubachallenge.jp/`; however, it is in Japanese.

[3]**Algorithm test_range_measurement** is presented in Table 8.5 and discussed in [5].

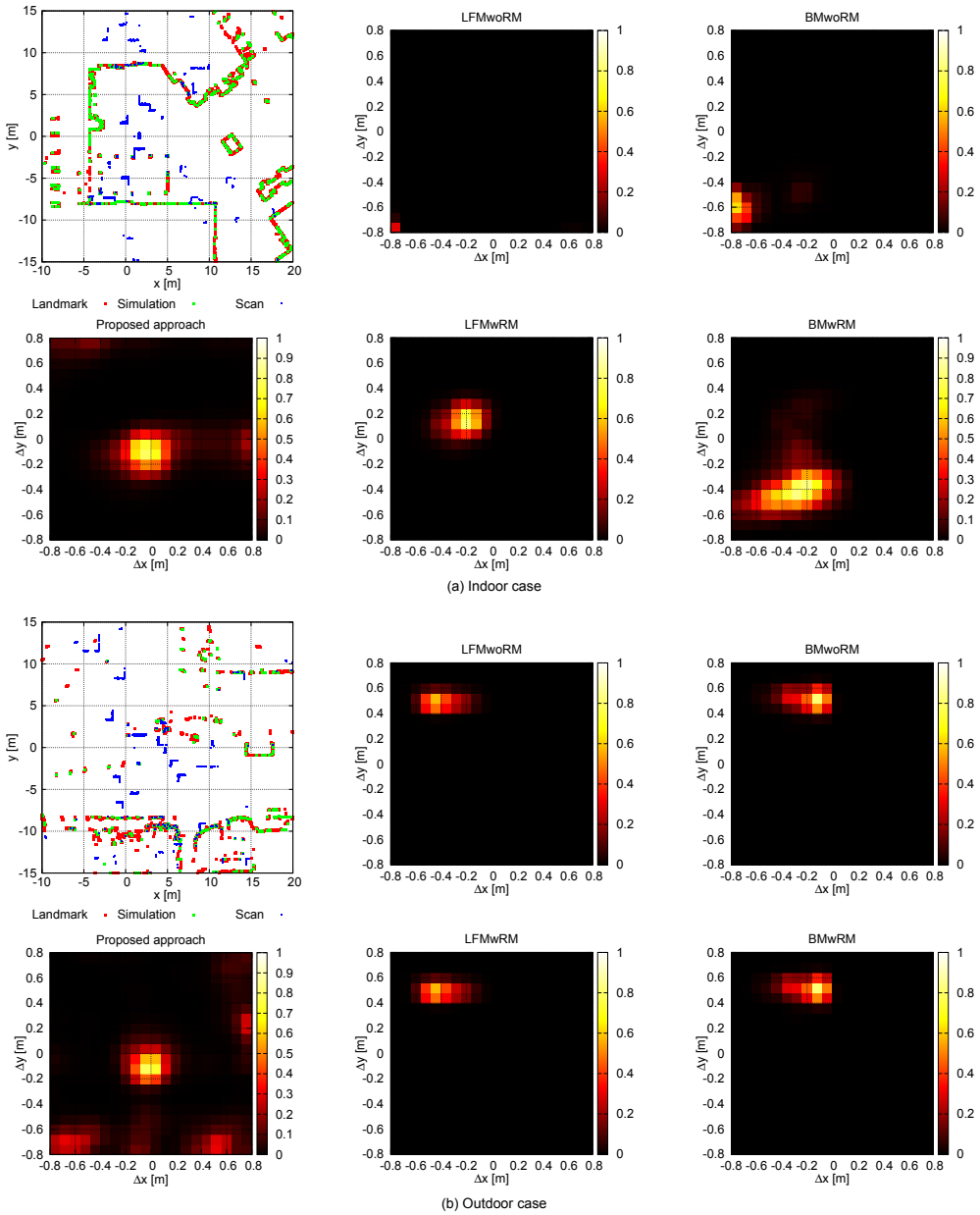

Fig. 5. Comparison results of the likelihood distributions. The top left figures show the simulated dynamic environment. The likelihood distribution generated using the proposed approach (bottom left) formed a peak around the ground truth in both cases, $(\Delta x, \Delta y) = (0, 0)$.

First, we describe the results shown in Fig. 5(a). The likelihood distributions shown in the top-middle and right figures were generated with the LFM and BM using all the scan points. It should be noted that the ground truth was set to origin $(\Delta x, \Delta y) = (0, 0)$, and heading direction θ was not changed in this experiment. The likelihood peak was moved from the origin in the two cases because of the environment dynamics. The likelihood distributions shown in the bottom-middle and right figures were generated using the remaining scan points after applying the rejection method with the LFM and BM. The performance of the models were better than that obtained when the rejection method is not applied; however, a small deviation from the origin was still seen in each case. The bottom-left figure shows the result obtained using the proposed approach and the peak of the likelihood is seen around the origin.

A similar trend can be seen in the results shown in Fig. 5(b). The likelihood distributions generated using LFM and BM were deviated from the origin, even after the rejection method was applied. Moreover, the likelihood distribution generated using the proposed approach formed the likelihood peak around the origin. However, the proposed approach also formed small peaks at some points that were deviated from the origin. This is because that the proposed approach could not uniquely determine the robot's pose due to the environment dynamics. This characteristic can be seen

in Fig. 3. Although this is a shortcoming of the proposed approach, it may be suitable for the position tracking localization problem, as it can form the peak of the likelihood distribution around the ground truth.

2) Classification performance: The proposed approach estimates the probability that categorizes the sensor observations as those obtained from mapped and unmapped obstacles. We evaluated this classification performance using simulations. Here, the i-th scan point is classified as that obtained from unmapped obstacles, when $p({}^{i}c_t = \text{unmapped}) \geq 0.9$ is satisfied. We also compared the proposed approach with the rejection method.

Figure 6 shows the two comparison results, in Figs. 6(a) and 6(b). First, we describe the top figure of both Figs. 6(a) and 6(b). In Fig. 6(a), the static landmarks were not removed from the simulation map shown with blue dots. Moreover, in Fig. 6(b), approximately 90 % of the static landmarks were removed from the simulation map. The simulated robot navigated this environment and performs localization using the proposed approach. The ground truth and estimated robot trajectory are represented with black and yellow lines. The red and green dots represent the scan points classified as mapped obstacles by the proposed approach and the rejection method, respectively. It should be noted that the rejection method was applied based on the particle distribution generated using the proposed approach.

Further, we describe the bottom figures of both Figs. 6(a) and 6(b). We could obtain the exact labels that enables us in identifying the scan points obtained from mapped and unmapped obstacles because we used simulation. By using these labels, we first computed the landmark rate that refers to the number of scan points obtained from mapped obstacles included in one observation, and it is represented with the blue line. Further, we computed the classification accuracy achieved by the proposed approach and the rejection method with the use of the labels and these are represented with red and green lines, respectively.

As shown in the top and bottom figures, the proposed approach will classify the scan points obtained from mapped obstacles. Its classification accuracy was always close to be 90 % in both cases. Thus, the proposed approach could localize the robot's trajectory even in highly dynamic environments. The classification performance of the rejection method was not higher than that of the proposed approach. The major cause of the low performance is the difficulty in parameter adjustment. The parameters used in the rejection method strongly depend on its performance, and these parameters should be determined from the data taken in the testing environment using the expectation maximization algorithm. However, determining these parameters accurately is not easy as the environment condition is not static. Moreover, the parameters used in the proposed approach do not strongly depend on its performance. Therefore, the proposed approach successfully worked.

In addition, the proposed approach could classify the scan points obtained behind the landmarks. The rejection method does not consider the removal of the landmarks; thus, it could not classify the scan points available behind the landmarks (see the top figure in Fig. 6(b)). The proposed approach could correspond to the scan points as it considers the environment

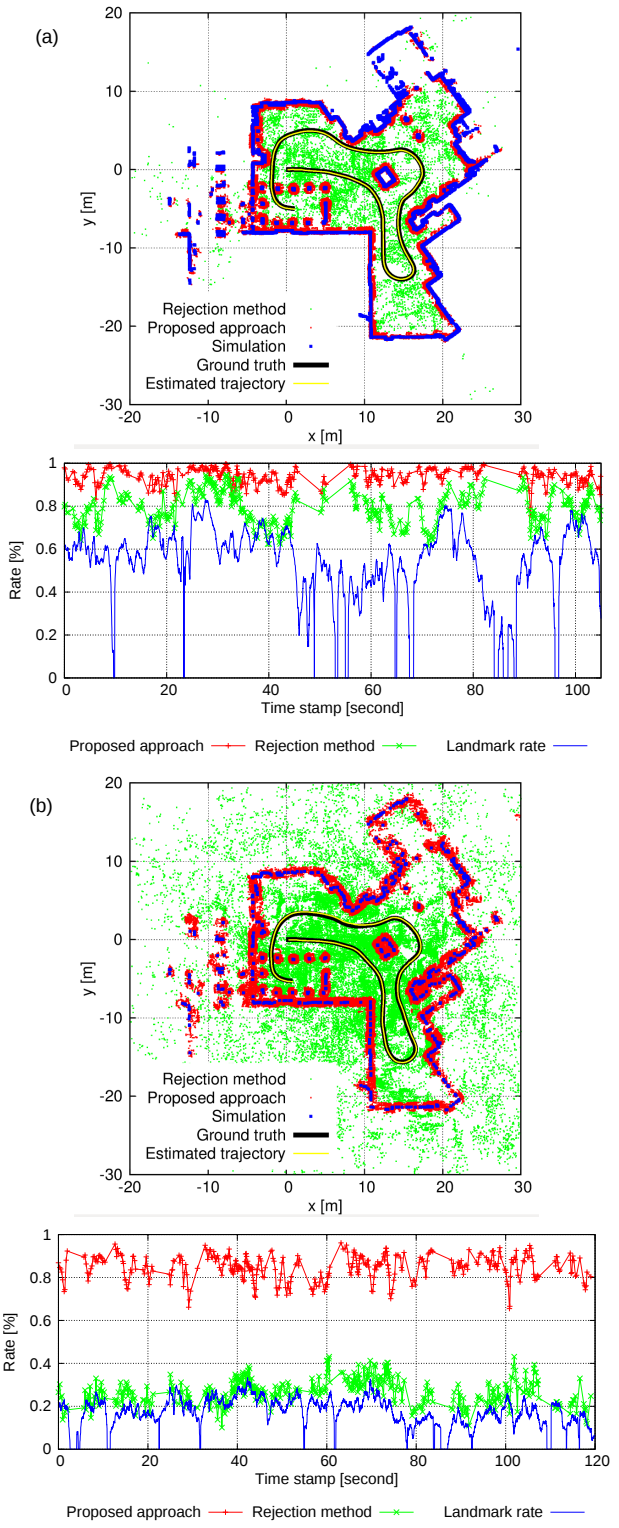

Fig. 6. Classification results considering the sensor observation class. The classification accuracy achieved by the proposed approach was approximately 90 %.

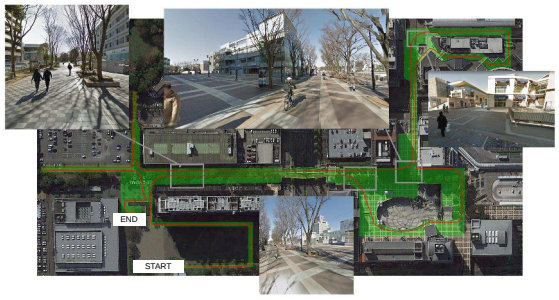

Fig. 7. Bird's eye view of the Tsukuba Challenge 2017's environment [31].

dynamics including the removal of the landmarks. Furthermore, the proposed approach has advantages in terms of the computation time. To apply the rejection method, we need to employ ray-tracing for each scan point, which takes a lot of computation time. Moreover, the proposed approach does not employ ray-tracing for the classification, and the scan point classification can be performed simultaneously while calculating the likelihood of the particles. Thus, the proposed approach does not increase the computation complexity.

D. Experiment in Tsukuba Challenge

Figure 7 shows a bird's eye view of the TC 2017's environment. The TC is a mobile robot navigation competition, in which navigating a pre-determined path of over 2 km in the real city environment is set as the task. We cannot modify the environment for the robots; thus, the robots should have robust navigation functions against the environment dynamics. We took the log data using the robot during the TC and tested the proposed approach off-line. To build a 2D consistent map, we applied a 3D LiDAR-based SLAM presented and discussed in [32].

1) Localization in entire areas: Figure 8 shows the localization result in the entire area. The left hand figure shows the estimated trajectory by the proposed approach. The top-right figure shows the fractions of valid (red) and matched (blue) scan points, where valid scan refers to the scan points that are hitting some obstacles and matched scan refers to the scan points plotted from the estimated pose that are matched with landmarks. The valid scan fraction describes the areas in which the robot is navigating. For example, A and C are wide open spaces, and the valid scan fraction is low. Moreover, B is a narrow space and the valid scan fraction could be high. As shown in the top-right figure, it could be seen that the robot navigated in various areas. In addition, the matched scan fraction is low in some areas because of the dynamic obstacles and noisy scan measurements. However, the proposed approach could localize the robot's trajectory.

As it is hard to obtain the ground truth of the robot's pose in wide environments, we could not evaluate the accuracy of the proposed approach. Instead, we uploaded a video showing the localization process on Internet, which can be seen at[4]. We hope that the video can be helpful for readers

[4]https://www.youtube.com/watch?v=3Vrj9N5Ai8o

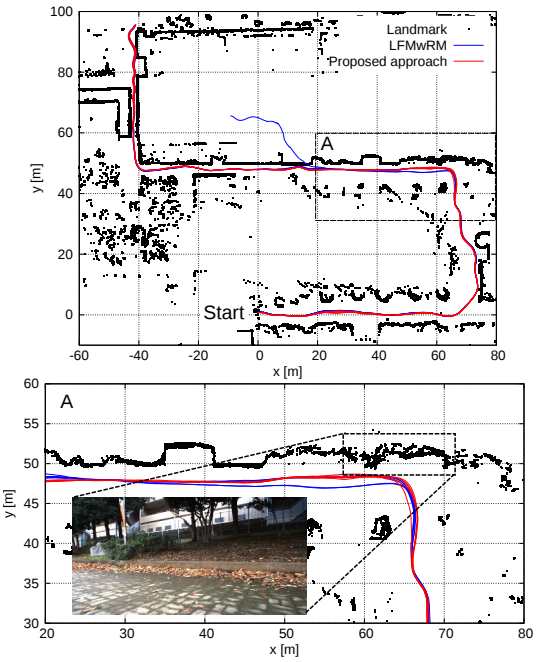

Fig. 9. Estimated trajectories by the proposed approach (red) and LFMwRM (blue) in the park environment.

to understand the performance of our proposed approach.

2) Localization in park: We considered that the most challenging environment for 2D LiDAR-based localization in the TC is the park environment around the start area, because there are irregular surfaces, such as bumps, grass, bushes, and trees in the park. The noisy scan measurements are often obtained due to the vibrations produced in the robot's roll and pitch angles. These noisy measurements sometimes cause localization failure. We tested the proposed approach and LFMwRM five times using the same log for verifying reproducibility.

Figure 9 depicts the estimated trajectories. LFMwRM failed its estimation once due to the noisy measurements. In addition, estimation results by LFMwRM did not have reproducibility in A. As can be seen the photo shown in the bottom, there are irregular surfaces, but the landmark map has a thin line. Thus, sometimes mismatches occur in the area. Moreover, the estimation results obtained by the proposed approach were converged in the area. Through the results, reproducibility of the proposed approach could be confirmed.

VI. Conclusion

This study has presented a mobile robot localization approach that considers the class of sensor observations, where "class" categorizes the sensor observations as those obtained from mapped and unmapped obstacles. To consider the class of the sensor observation, we propose an observation model that simultaneously estimates the robot's pose and the sensor observation class. By estimating the class and robot's pose simultaneously, localization can be performed using the sensor observations obtained only from

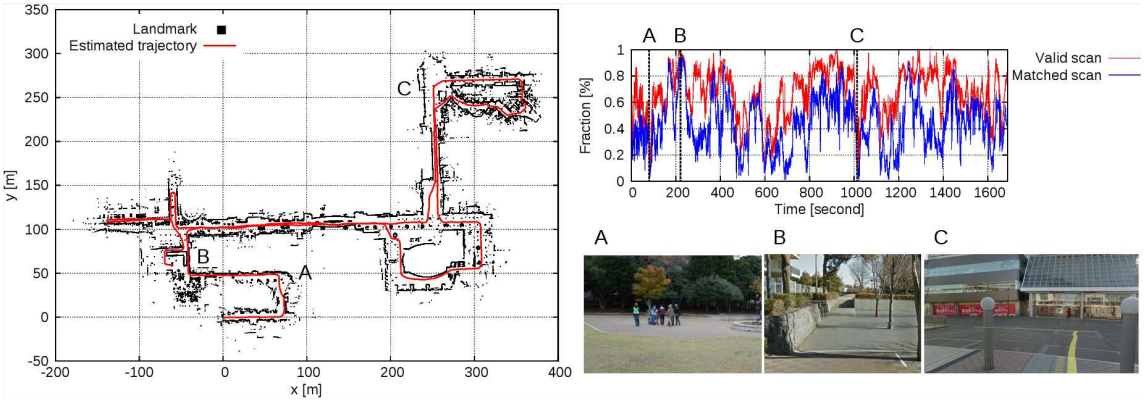

Fig. 8. Localization result in the entire areas (left), fractions of valid and matched scan points (top right), and example scene of the navigation environment (bottom right).

mapped obstacles. As a result, localization robustness against environment dynamics is improved in robots. The robustness of the proposed approach against environment dynamics is verified through experiments using simulated and actual robots. The source code related to this study is available at `https://github.com/NaokiAkai/AutoNavi`.

Our future study will be based on applying the proposed localization approach to another case, in which the reference map may contain some semantics. For example, in an autonomous car's localization problem, a road marker map is available. In this map, at least two semantics (class) are included, i.e., ground surface and marker. The proposed approach of this study might be effective in simultaneously estimating the semantics and the car's pose.

ACKNOWLEDGMENT

This study was supported by the Center of Innovation Program (Nagoya-COI) funded by the Japan Science and Technology Agency and Technology Agency and Artificial Intelligence Research Promotion Foundation.

REFERENCES

[1] L. Y. Morales *et al.*, "Autonomous robot navigation in outdoor cluttered pedestrian walkways," *JFR*, vol. 26, no. 8, pp. 609–635, 2009.
[2] R. Kümmerle *et al.*, "Autonomous robot navigation in highly populated pedestrian zones," *JFR*, vol. 32, no. 4, pp. 565–589, 2015.
[3] N. Akai *et al.*, "Autonomous driving based on accurate localization using multilayer LiDAR and dead reckoning," in *Proc. IEEE ITSC*, pp. 1147–1152, 2017.
[4] F. Dellaert *et al.*, "Monte Carlo localization for mobile robots," in *Proc. IEEE ICRA*, vol. 2, pp. 1322–1328, 1999.
[5] S. Thrun *et al.*, "Probabilistic robotics," *MIT Press*, 2005.
[6] D. Fox *et al.*, "Markov localization for mobile robots in dynamic environments," *JAIR*, vol. 11, pp. 391–427, 1999.
[7] W. Burgard *et al.*, "Experiences with an interactive museum tour-guide robot," *Artificial Intelligence*, vol. 114, no. 1–2, pp. 3–55, 1999.
[8] M. Montemerlo *et al.*, "Conditional particle filters for simultaneous mobile robot localization and people-tracking," in *Proc. IEEE ICRA*, 2002.
[9] D. Anguelov *et al.*, "Learning hierarchical object maps of non-stationary environments with mobile robots," *UAI*, 2002.
[10] D. Hähnel *et al.*, "Map building with mobile robots in dynamic environments," in *Proc. IEEE ICRA*, 2003.
[11] D. Schulz *et al.*, "People tracking with anonymous and ID-sensors using Rao-Blackwellised particle filters," in *Proc. IJCAI*, pp. 921–926, 2003.
[12] S. Olufs *et al.*, "An efficient area-based observation model for Monte-Carlo robot localization," in *Proc. IEEE/RSJ IROS*, pp. 13–20, 2009.
[13] E. Takeuchi *et al.*, "Robust localization method based on free-space observation model using 3D-map," in *Proc. IEEE ROBIO*, pp. 973–979, 2010.
[14] D. F. Wolf *et al.*, "Mobile robot simultaneous localization and mapping in dynamic environments," *Autonomous Robots*, vol. 19, no. 1, pp. 53–65, 2005.
[15] L. Montesano *et al.*, "Modeling the static and the dynamic parts of the environment to improve sensor-based navigation," in *Proc. IEEE ICRA*, 2005.
[16] P. Biber *et al.*, "Dynamic maps for long-term operation of mobile service robots," in *Proc. RSS*, 2005.
[17] C. -C. Wang *et al.*, "Simultaneous localization, mapping and moving object tracking," *IJRR*, vol. 26, no. 9, pp. 889–916, 2007.
[18] G. Gallagher *et al.*, "GATMO: A generalized approach to tracking movable objects," in *Proc. IEEE ICRA*, 2009.
[19] C. Chen *et al.*, "Dynamic environment modeling with gridmap: A multiple-object tracking application," in *Proc. IEEE ICARCV*, 2006.
[20] S. Brechtel *et al.*, "Recursive importance sampling for efficient grid-based occupancy filtering in dynamic environments," in *Proc. IEEE ICRA*, 2010.
[21] D. Meyer-Delius *et al.*, "Occupancy grid models for robot mapping in changing environments," in *Proc. AAAI*, pp. 2024–2030, 2012.
[22] J. Saarinen *et al.*, "Independent Markov chain occupancy grid maps for representation of dynamic environments," in *Proc. IEEE/RSJ IROS*, 2012.
[23] D. Avots *et al.*, "A probabilistic technique for simultaneous localization and door state estimation with mobile robots in dynamic environments," in *Proc. IEEE/RSJ IROS*, 2002.
[24] A. Petrovskaya *et al.*, "Probabilistic mobile manipulation in dynamic environments, with application to opening doors," in *Proc. IJCAI*, 2007.
[25] C. Stachniss *et al.*, "Mobile robot mapping and localization in non-static environments," in *Proc. AAAI*, 2005.
[26] A. Milstein, "Dynamic maps in Monte Carlo localization," *Advances in Artificial Intelligence*, vol. 3501, pp. 1–12, 2005.
[27] G. D. Tipaldi *et al.*, "Lifelong localization in changing environments," *IJRR*, vol. 32, no. 14, pp. 1662–1678, 2013.
[28] R. Valencia *et al.*, "Localization in highly dynamic environments using dual-timescale NDT-MCL," in *Proc. IEEE ICRA*, 2014.
[29] D. Meyer-Delius *et al.*, "Temporary maps for robust localization in semi-static environments," in *Proc. IEEE/RSJ IROS*, 2010.
[30] S. -W. Yang *et al.*, "Feasibility grids for localization and mapping in crowded urban scenes," in *Proc. IEEE ICRA*, 2011.
[31] J. Lambert *et al.*, "Tsukuba challenge 2017 dynamic object tracks dataset for pedestrian behavior analysis," *JRM*, 2018 (accepted).
[32] E. Takeuchi *et al.*, "A 3-D scan matching using improved 3-D normal distributions transform for mobile robotic mapping," in *Proc. IEEE/RSJ IROS*, pp. 3068–3073, 2006.

View publication stats